Preprints of the 21st IFAC World Congress (Virtual)
Berlin, Germany, July 12-17, 2020

Complex-valued sliding mode control of an induction motor ⋆

A. Dòria-Cerezo * **J.M. Olm** * **V. Repecho** * **D. Biel** *

* *Inst. of Industrial and Control Engineering, Universitat Politècnica de Catalunya, Spain (e-mail: arnau.doria@upc.edu).*

Abstract: Three-phase induction motors admit a complex-valued space state representation. In this paper, this complex description is used to design a torque controller and a rotor flux observer based on sliding modes. The advantage of using the complex representation is an order reduction of the system and a simplification of the analysis. The obtained results are illustrated by means of numerical simulations.

Keywords: Sliding mode control, sliding mode observer, complex-valued nonlinear systems, induction motor, torque control

1. INTRODUCTION

1.1 Motivation

The representation of physical systems using complex-valued dynamical models was proposed for induction machines (Novotny and Wouterse (1976)) and for three-phase electrical systems (Harnefors (2007)), in general. Recent papers have proposed the complex-valued modelling for representing electrical systems, with the advantage of reducing the order of the systems and facilitate the control design. These papers include both electrical machines (Dòria-Cerezo et al. (2013), Baesmat and Bodson (2019) and Bodson (2019)) and power converters (Dòria-Cerezo and Bodson (2016) and Dòria-Cerezo et al. (2019)), but all of them are limited to linear systems.

The induction motor is a three-phase electrical machine widely used in the industry as servo applications due to its relatively low cost, less maintenance, and robustness. Three-phase voltage and currents (abc) can be represented, without loss of generalization, into the so-called $\alpha\beta$ framework that allows to reduce the order and to simplify the dynamics of the electrical equations. The control of induction motors is, inherently, a nonlinear phenomena because the electromechanical conversion. Usually, this nonlinear characteristic is overcome using the rotor flux oriented control (Leonhard (2001)), known as Field Oriented Control (FOC), which proposes a reference framework that allows, after regulating the rotor flux, a linear behaviour.

Sliding modes have been largely applied to induction motors, from control (Utkin et al. (1999)) to observation; see some recent works in (Wang et al. (2018)), (Morawiec and Lewicki (2019) or (Holakooie et al. (2019)). However, the use of sliding modes for complex-valued dynamical systems has not been reported so far.

⋆ The work was partially supported by the Government of Spain through the *Agencia Estatal de Investigación* Project DPI2017-85404-P and by the *Generalitat de Catalunya* through the Project 2017 SGR 872.

1.2 Contributions

This paper presents a complex-valued sliding mode control-based algorithm that encompasses both torque control and a rotor flux observer. The main advantage of using the complex-based approach is order reduction; from two ($\alpha\beta$) components, to one complex value that simplifies the synthesis and the analysis of the control algorithm and observer algorithms.

From a practical point of view, and differently from other papers based on FOC, the adopted induction motor control algorithm comes from the $\alpha\beta$ coordinates. This choice allows disregarding the rotor flux regulation as a secondary control objective offering other alternatives than FOC, such as field weakening or minimising the losses in the stator windings.

Notation. $j = \sqrt{-1}$ is used, instead of i, to avoid confusion with electrical currents used in the application examples; $\mathbb{C}^n$ denotes the complex nth-dimensional space; $\mathrm{Re}(z)$ and $\mathrm{Im}(z)$ denote the real and imaginary parts, respectively, of $z \in \mathbb{C}$; z^* denotes the conjugate of $z \in \mathbb{C}$; $|z|$ and δ_z denote the magnitude and phase, respectively, of $z \in \mathbb{C}$; $\mathrm{sign}(z)$ denotes the sign function of a complex value $z \in \mathbb{C} \setminus \{0\}$, which is computed as in (Bachman and Narici (1966)):

$$\mathrm{sign}(z) = \frac{z}{|z|}.$$

2. COMPLEX-VALUED MODEL OF AN INDUCTION MOTOR

Consider a three-phase electrical variable (voltage or current) given by $x(t) = (x_a(t), x_b(t), x_c(t))$. The transformation of three-phase electrical variables ($x(t)$) to complex-valued variables ($z(t)$) is defined by

$$z(t) = c\left(1, e^{-j\frac{2\pi}{3}}, e^{j\frac{2\pi}{3}}\right)\begin{pmatrix} x_a(t) \\ x_b(t) \\ x_c(t) \end{pmatrix}, \qquad (1)$$

where different values of c correspond to different choices. In this paper we adopt the power preserving choice, i.e., $c = 1$.

2.1 Complex vector representation

A complex vector representation of the inductor motor is widely developed in Chapter 2 of (Novotny and Lipo (1996)). The dynamics of the inductor motor after applying the complex transformation (1) is governed by:

$$L_s\frac{\mathrm{d}i_s}{\mathrm{d}t} + M\frac{\mathrm{d}}{\mathrm{d}t}\left(i_r e^{jn_p\theta}\right) = -R_s i_s + u_s \tag{2a}$$

$$M\frac{\mathrm{d}}{\mathrm{d}t}\left(i_s e^{-jn_p\theta}\right) + L_r\frac{\mathrm{d}i_r}{\mathrm{d}t} = -R_r i_r \tag{2b}$$

$$J\frac{\mathrm{d}\omega}{\mathrm{d}t} = -b\omega + \tau_e - \tau_L \tag{2c}$$

where $i_s, i_r \in \mathbb{C}$ are the stator and rotor currents; $\omega, \theta \in \mathbb{R}$ are the mechanical speed and the rotor position, respectively; $u_s \in \mathbb{C}$ is the stator voltage, which is used as a control input; $L_s, L_r, M \in \mathbb{R}^+$ are the stator, rotor and mutual inductances; $R_s, R_r \in \mathbb{R}^+$ are the stator and rotor resistances modelling the inductor losses; $J \in \mathbb{R}^+$ is the rotor inertia, $b \in \mathbb{R}^+$ is the damping coefficient; $n_p \in \mathbb{N}$ is the number of pole pairs; $\tau_L \in \mathbb{R}$ is the load torque, and $\tau_e \in \mathbb{R}$ is the electromagnetic torque

$$\tau_e = n_p M \mathrm{Im}\left(i_s\left(i_r e^{jn_p\theta}\right)^*\right). \tag{3}$$

2.2 Rotor flux model

Similarly to (Chiasson (2005)), and defining the rotor flux linkage as

$$\psi_r = Mi_s + L_r i_r e^{jn_p\theta},$$

where $\psi_r \in \mathbb{C}$, (2a)-(2b) can be written as

$$\mu L_s\frac{\mathrm{d}i_s}{\mathrm{d}t} + \frac{M}{L_r}\frac{\mathrm{d}\psi_r}{\mathrm{d}t} = -R_s i_s + u_s \tag{4a}$$

$$\frac{\mathrm{d}\psi_r}{\mathrm{d}t} = \frac{R_r M}{L_r} i_s - \left(\frac{R_r}{L_r} - jn_p\omega\right)\psi_r, \tag{4b}$$

where $\mu = 1 - \frac{M^2}{L_s L_r}$ is known as the leakage factor, and the electromagnetic torque results in

$$\tau_e = \kappa \mathrm{Im}\left(i_s\psi_r^*\right), \tag{5}$$

with $\kappa = n_p\frac{M}{L_r}$. Equations (4a)-(4b) can be written in a more compact way as

$$\frac{\mathrm{d}i_s}{\mathrm{d}t} = -\gamma i_s + \beta\left(\eta - jn_p\omega\right)\psi_r + \frac{1}{\mu L_s}u_s \tag{6a}$$

$$\frac{\mathrm{d}\psi_r}{\mathrm{d}t} = -\left(\eta - jn_p\omega\right)\psi_r + \eta M i_s, \tag{6b}$$

where $\gamma = \frac{R_s}{\mu L_s} + \frac{R_r M^2}{\mu L_s L_r^2}$, $\beta = \frac{M}{\mu L_s L_r}$ and $\eta = \frac{R_r}{L_r}$ is known as the rotor time constant.

The main advantage of model (6) with respect to the one in (2) is that the explicit dependency on the angular position, θ, is removed.

3. CONTROL DESIGN

The control objective in electrical motors is to set one mechanical variable (position, speed or torque) to its desired value. In this paper, a control torque strategy for tracking the electromechanical torque is proposed, and the position/speed control is left to outer loops.

3.1 Complex switching function

Inspired in (5), the following sliding manifold is proposed:

$$\sigma = \kappa i_s\psi_r^* - \alpha_d = 0, \tag{7}$$

where $\alpha_d \in \mathbb{C}$ is a constant value such that its imaginary part is the desired torque, namely $\mathrm{Im}(\alpha_d) = \tau_e^d$,

$$\alpha_d = \mathrm{Re}(\alpha_d) + j\tau_e^d, \tag{8}$$

while the real part of α_d will be used for secondary purposes, see details in Section 3.5. Notice, finally, that the simplest choice $\sigma = \kappa\mathrm{Im}\left(i_s\psi_r^*\right) - \tau_e^d$ as switching function is not holomorphic.

3.2 Complex sliding mode controller

The equivalent control, u_{eq}, is defined as the control input guaranteeing $\dot{\sigma} = 0$. Differentiating (7) with respect to time yields

$$\dot{\sigma} = \kappa\left(\psi_r^*\frac{\mathrm{d}i_s}{\mathrm{d}t} + i_s\frac{\mathrm{d}\psi_r^*}{\mathrm{d}t}\right).$$

Taking into account (6) and after some algebra one obtains

$$\frac{1}{\mu L_s}\psi_r^* u_{eq} = -\eta M|i_s|^2 - \beta\left(\eta - jn_p\omega\right)|\psi_r|^2 + \left(\gamma + \eta + jn_p\omega\right)i_s\psi_r^*. \tag{9}$$

Consider the Lyapunov function candidate

$$V = \frac{1}{2}\sigma^*\sigma. \tag{10}$$

Using the definition of equivalent control in (9), the time derivative of (10) can be written as:

$$\dot{V} = \mathrm{Re}\left(\sigma^*\frac{\kappa}{\mu L_s}\psi_r^*(u_s - u_{eq})\right) \tag{11}$$

Then, with the switching control policy [1]

$$u_s = -2V_{dc}\frac{\sigma\psi_r}{|\sigma\psi_r|} = -2V_{dc}\mathrm{sign}(\sigma\psi_r), \tag{12}$$

where $V_{dc} \in \mathbb{R}$, (11) results in:

$$\begin{aligned}
\dot{V} &= -\mathrm{Re}\left(\sigma^*\frac{\kappa}{\mu L_s}\psi_r^*\left(2V_{dc}\frac{\sigma\psi_r}{|\sigma\psi_r|} + u_{eq}\right)\right)\\
&= -\frac{\kappa}{\mu L_s}\mathrm{Re}\left(\sigma^*\psi_r^*\left(2V_{dc}\frac{\sigma\psi_r}{|\sigma\psi_r|} + u_{eq}\right)\right)\\
&= -\frac{\kappa}{\mu L_s}\mathrm{Re}\left(|\sigma||\psi_r|2V_{dc} + u_{eq}\sigma^*\psi_r^*\right)\\
&= -\frac{\kappa}{\mu L_s}|\sigma||\psi_r|\mathrm{Re}\left(2V_{dc} + u_{eq}\frac{\sigma^*\psi_r^*}{|\sigma||\psi_r|}\right)\\
&= -\frac{\kappa}{\mu L_s}|\sigma||\psi_r|\mathrm{Re}\left(2V_{dc} + |u_{eq}|e^{j(\delta_{eq}-\delta_\sigma-\delta_{\psi_r})}\right)\\
&= -\frac{\kappa}{\mu L_s}|\sigma||\psi_r|\left(2V_{dc} + |u_{eq}|\cos(\delta_{eq}-\delta_\sigma-\delta_{\psi_r})\right),
\end{aligned} \tag{13}$$

and sliding motion occurs on $\sigma = 0$ whenever

$$2V_{dc} > |u_{eq}| \tag{14}$$

and $|\psi_r| \neq 0$.

[1] The selection of $2V_{dc}$ as the control gain is because the complex transformation in (1) with $c = 1$ projects the three-phase values with amplitude V_{dc} on a circumference of radius $2V_{dc}$ in the complex plane.

3.3 Finite time convergence

The switched control strategy in (12) ensures that the sliding manifold (7) is reached in finite time. In order to support this statement, let us assume that

$$\frac{\kappa}{\mu L_s}|\psi_r| \geq \epsilon_1$$
$$2V_{dc} - |u_{eq}| > \epsilon_2,$$

with $\epsilon_1, \epsilon_2 \in \mathbb{R}^+$. Then, $\dot{V}$ in (13) can be bounded as follows:

$$\dot{V} \leq -\epsilon_1\epsilon_2|\sigma|; \tag{15}$$

moreover, setting

$$\xi = \sqrt{2}\epsilon_1\epsilon_2 > 0$$

(15) results in

$$\dot{V} \leq -\xi V^{\frac{1}{2}}.$$

It follows that $V(t) = 0$ for $t \geq T$, with

$$T = \frac{2}{\xi}\sqrt{V(0)},$$

so $\sigma = 0$ is reached in finite time.

3.4 Ideal sliding dynamics

The ideal sliding dynamics occurs when $\dot{\sigma} = \sigma = 0$. This allows to replace (6a) by (7). In turn, as from (7) one has that

$$e^{j(\delta_{i_s} - \delta_{\psi_r})} = \frac{1}{\kappa|i_s||\psi_r|}\alpha_d,$$

the ideal sliding dynamics, here given by (6b), can be written as

$$\frac{\mathrm{d}|\psi_r|}{\mathrm{d}t} + j|\psi_r|\frac{\mathrm{d}\delta_{\psi_r}}{\mathrm{d}t} = -(\eta - jn_p\omega)|\psi_r| + \alpha_d\frac{\eta M}{\kappa}\frac{1}{|\psi_r|}, \tag{16}$$

which does not depend on the stator current dynamics. Then, the real part of the complex dynamics (16) boils down to:

$$\frac{\mathrm{d}|\psi_r|}{\mathrm{d}t} = -\eta|\psi_r| + \mathrm{Re}(\alpha_d)\frac{\eta M}{\kappa}\frac{1}{|\psi_r|}.$$

This dynamics is asymptotically stable [2], which reveals that the rotor flux stabilises at the equilibrium value

$$|\psi_r^\star|^2 = \frac{M}{\kappa}\mathrm{Re}(\alpha_d) = \frac{L_r}{n_p}\mathrm{Re}(\alpha_d), \tag{17}$$

where $\mathrm{Re}(\alpha_d) > 0$.

The imaginary part of the ideal sliding dynamics (16) provides the rotating frequency of the rotor flux, ω_s. Using (17) into the imaginary components of (16) one gets

$$\omega_s := \frac{\mathrm{d}\delta_{\psi_r}}{\mathrm{d}t} = \eta\frac{\mathrm{Im}(\alpha)}{\mathrm{Re}(\alpha)} + n_p\omega.$$

Then, from $\sigma = 0$ in (7) and assuming that the rotor flux reaches its steady state,

$$\kappa|i_s^\star|e^{j\delta_{i_s}}|\psi_r^\star|e^{-j\delta_{\psi_r}} = \alpha_d,$$

this yielding

$$\delta_{i_s} = \delta_{\psi_r} + \delta_{\alpha_d}$$
$$|i_s^\star| = \frac{|\alpha_d|}{\kappa|\psi_r^\star|}.$$

[2] This can straightforwardly proved by using $V(x) = \frac{1}{2}(x - x^\star)^2$ as a Lyapunov function candidate.

Finally, using (17) the equilibrium of the modulus of the stator currents is

$$|i_s^\star|^2 = \frac{|\alpha_d^2|}{\kappa M\mathrm{Re}(\alpha_d)}. \tag{18}$$

3.5 Design of $Re(\alpha_d)$

The design of the sliding manifold (8) allows to set different values for the real part of α_d in (8).

On the one hand, and similarly to FOC, from (17) the rotor flux control can be achieved by setting

$$\mathrm{Re}(\alpha_d) = \frac{n_p}{L_r}|\psi_r^d|^2. \tag{19}$$

Additionally, a further analysis of the stator currents steady state reveals that $\mathrm{Re}(\alpha_d)$ can be used to minimise the stator currents amplitude and, consequently, to increase the motor efficiency by reducing the losses by the Joule's effect. It follows from (18) that

$$|i_s^\star|^2 = \frac{\mathrm{Re}(\alpha_d)^2 + \mathrm{Im}(\alpha_d)^2}{\kappa M\mathrm{Re}(\alpha_d)},$$

and the value that minimises $|i_s^\star|^2$ can be obtained from

$$\frac{\partial|i_s^\star|^2}{\partial\mathrm{Re}(\alpha_d)} = \frac{\mathrm{Re}(\alpha_d)^2 - \mathrm{Im}(\alpha_d)^2}{\kappa M\mathrm{Re}(\alpha_d)^2} = 0,$$

which implies that

$$\mathrm{Re}(\alpha_d) = \mathrm{Im}(\alpha_d), \tag{20}$$

the minimum current being

$$|i_s^{\star\min}|^2 = \frac{2}{\kappa M}\mathrm{Im}(\alpha).$$

Then the selection of (20) ensures the minimum losses in the stator resistances.

Finally, other options can be explored, such as enlarging the sliding motion region given in (14) by reducing the equivalent control absolute value from (9). This approach would be similar to the well-known field weakening strategy.

4. OBSERVER DESIGN

The observation of the rotor flux is necessary in any control scheme of induction motors. Using the complex vector representation it is possible to design an algorithm capable of estimating the rotor flux.

Assuming that all the parameters are known and that the mechanical speed is measurable the observer equations are, similarly to (Drakunov and Utkin (1995)),

$$\frac{\mathrm{d}\hat{i}_s}{\mathrm{d}t} = -\gamma i_s + \beta(\eta - jn_p\omega)\hat{\psi}_r + \frac{1}{\mu L_s}u_s - \nu \tag{21a}$$

$$\frac{\mathrm{d}\hat{\psi}_r}{\mathrm{d}t} = -(\eta - jn_p\omega)\hat{\psi}_r + \eta M i_s + l\nu, \tag{21b}$$

where

$$\nu = \rho\frac{\hat{i}_s - i_s}{|\hat{i}_s - i_s|} = \rho\ \mathrm{sign}(\hat{i}_s - i_s), \tag{22}$$

$l \in \mathbb{C}$ and $\rho \in \mathbb{R}$. Let us define

$$\tilde{i}_s = \hat{i}_s - i_s$$
$$\tilde{\psi}_r = \hat{\psi}_r - \psi_r.$$

From (6a) and (21a), the dynamics of $\tilde{i}_s$ results in

$$\frac{\mathrm{d}\tilde{i}_s}{\mathrm{d}t} = \beta\left(\eta - jn_p\omega\right)\tilde{\psi}_r - \rho\,\mathrm{sign}(\tilde{i}_s).$$

Then, considering $V_o = \frac{1}{2}\tilde{i}_s^*\tilde{i}_s$ as a Lyapunov function candidate, its time derivative is given by:

$$\begin{aligned}\dot{V}_o &= \mathrm{Re}\left(\tilde{i}_s^*\dot{\tilde{i}}_s\right)\\ &= \mathrm{Re}\left(\tilde{i}_s^*\left(\beta\left(\eta - jn_p\omega\right)\tilde{\psi}_r - \rho\frac{\tilde{i}_s}{|\tilde{i}_s|}\right)\right)\\ &= \mathrm{Re}\left(\beta\left(\eta - jn_p\omega\right)\tilde{i}_s^*\tilde{\psi}_r - \rho|\tilde{i}_s|\right)\\ &= -|\tilde{i}_s|\mathrm{Re}\left(\rho - \beta\left(\eta - jn_p\omega\right)\tilde{\psi}_r\frac{\tilde{i}_s^*}{|\tilde{i}_s|}\right)\\ &= -|\tilde{i}_s|\mathrm{Re}\left(\rho - \beta|\psi_r|\left(\eta - jn_p\omega\right)e^{j(\delta_{\tilde{\psi}_s} - \delta_{\tilde{i}_s})}\right)\end{aligned}$$

Then, if

$$\rho > \beta|\tilde{\psi}_r|\sqrt{\eta^2 + n_p^2\omega^2} \geq \epsilon_o$$

with $\epsilon_o \in \mathbb{R}$, one gets

$$\dot{V}_o \leq -\epsilon_o|\tilde{i}_s|$$

and $\tilde{i}_s$ converges to zero in finite time.

During sliding motion it is $\tilde{i}_s = \dot{\tilde{i}}_s = 0$; hence,

$$0 = \beta\left(\eta - jn_p\omega\right)\tilde{\psi}_r - \nu_{eq} \tag{23}$$

$$\frac{\mathrm{d}\tilde{\psi}_r}{\mathrm{d}t} = -\left(\eta - jn_p\omega\right)\tilde{\psi}_r + l\nu_{eq}, \tag{24}$$

and replacing (23) in (24) yields

$$\frac{\mathrm{d}\tilde{\psi}_r}{\mathrm{d}t} = -\left(\eta - jn_p\omega\right)(1 - l\beta)\tilde{\psi}_r. \tag{25}$$

which is stable since

$$-\eta(1 - \mathrm{Re}(l)\beta) + \mathrm{Im}(l)\beta n_p\omega < 0.$$

Therefore, if the the motor does not change the direction of rotation, the selection

$$\mathrm{Re}(l) < \frac{1}{\beta}$$
$$\mathrm{sign}\left(\mathrm{Im}(l)\right) = -\mathrm{sign}(\omega)$$

ensures that the reduced order complex motion (25) is stable.

5. NUMERICAL SIMULATIONS

5.1 Hysteresis implementation

Similarly to the standard sliding mode control approach, ideal complex sliding modes require infinite switching frequency, but this feature is unavailable in practical applications. For the numerical implementation an hysteresis approach strategy is proposed to approximate the complex sign functions in (12) and (21).

The hysteresis approximation for the complex sign function is defined as a ball of radius ϵ_h in the complex plane representation of σ where the output state is remembered. Out of this area, the complex function is evaluated. The hysteresis for the complex function (12) is implemented as shown in Algorithm 1, where p refers to each iteration.

A ball of radius ϵ_{ho} is analogously implemented for (22).

Algorithm 1 Algorithm for a complex hysteresis

Input: $\sigma_p, u_{p-1}, \epsilon_h, k$
Output: u_p
1: **if** $(|\sigma_p| < \epsilon_h)$ **then**
2: $\quad u_p = u_{p-1}$
3: **else**
4: $\quad u_p = -k\frac{\sigma_p}{|\sigma_p|}$
5: **end if**
6: **return** u_p

5.2 Simulation results

Numerical simulation have been run to test the control law in (7) and (12) and the observer proposed in (21)-(22), see the complete control scheme in Figure 1.

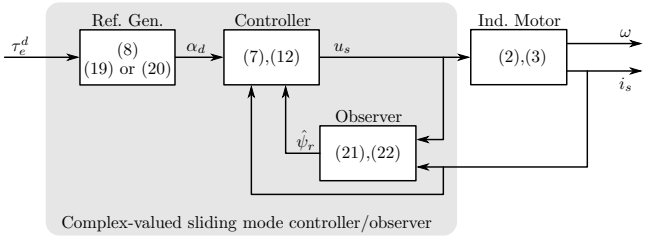

Fig. 1. Overall control scheme.

The used induction motor was a three pole-pairs machine with the following parameters: $L_s = L_r = 109.3$mH, $M = 100$mH, $R_s = 2.7\Omega$, $R_r = 0.5\Omega$, $J = 0.001$kg·m^2, $b = 0.001$N·m·s., and $V_{dc} = 400$V.

The desired torque is obtained from an outer PI controller that has been added to regulate the mechanical speed to a desired value, ω_d. The PI controller gains were $k_p = 0.05$ and $k_i = 7.5$, the observer gains were $l = -(0.5 + j0.1)$ and $\rho = 10^5$, and the hysteresis radii were $\epsilon_h = 0.1$ and $\epsilon_{ho} = 0.05$. Finally, α_d has been computed as proposed in (20), so a minimum stator current is ensured.

The simulated test consists in starting at $\omega(0) = 0$ regulating the mechanical speed at $\omega_d = 100$rad/s. At $t = 0.25$s, a disturbance external torque $\tau_L = 0.15$N·m is connected.

Figures 2 and 3 show the obtained dynamics. The required torque provided by the PI controller is perfectly tracked by the complex-valued sliding controller (see the second plot in Figure 2), so the mechanical speed is also regulated. Figure 3 shows the complex-valued switching function. The hysteresis area defined by a ball of radius ϵ_h is obtained when the switching function is plotted in the complex plane.

The observer behaviour is shown in Figures 4 and 5. The obtained results show that the observation of the rotor-flux is achieved thanks to the sliding motion induced on the absolute error observation of the stator currents, $\tilde{i}_s$, see the second plot in Figure 4. Similarly to Figure 3, the hysteresis approximation defined by a ball of radius ϵ_{ho} is observed in Figure 5 as well.

6. CONCLUSION

Complex-valued sliding modes have been proposed for the control and observation of an induction motor. This ap-

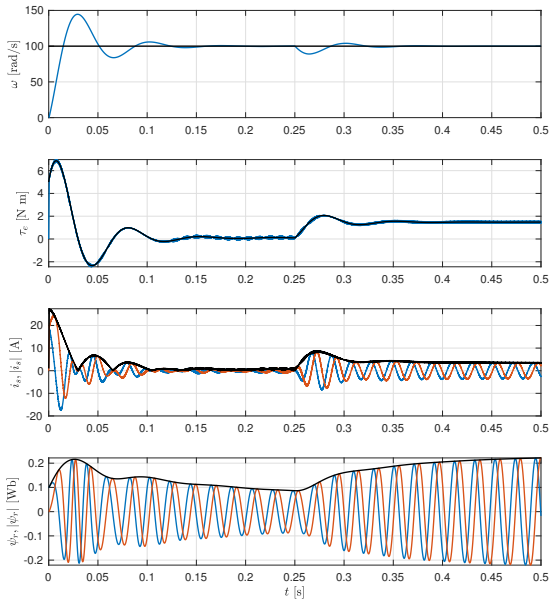

Fig. 2. Simulation results: Speed/torque control. From top to bottom: mechanical speed (blue) and its desired value (black) ω, ω_d; electromechanical torque (blue) and its desired value (black), τ_e, τ_e^d; real and imaginary parts of the stator current (blue, red) and its absolute value (in black), i_s, $|i_s|$; real and imaginary parts of the rotor flux (blue,red) and its absolute value (in black), ψ_r, $|\psi_r|$.

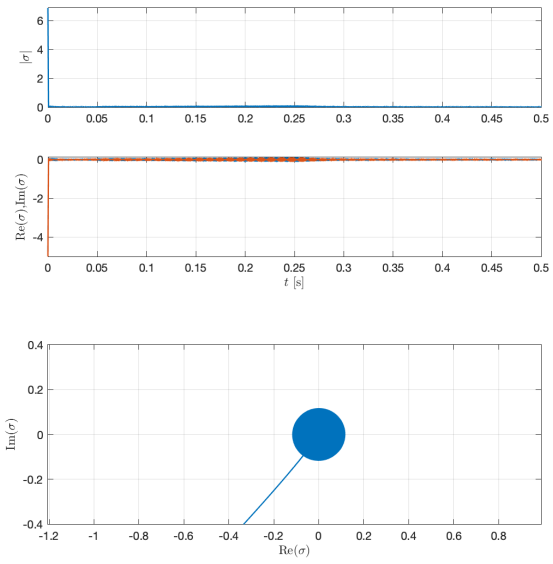

Fig. 3. Simulation results: Speed/torque control. From top to bottom: absolute value of the switching function, $|\sigma|$; real and imaginary parts of the switching function (in blue and red, respectively); complex plane plot of the switching function, σ.

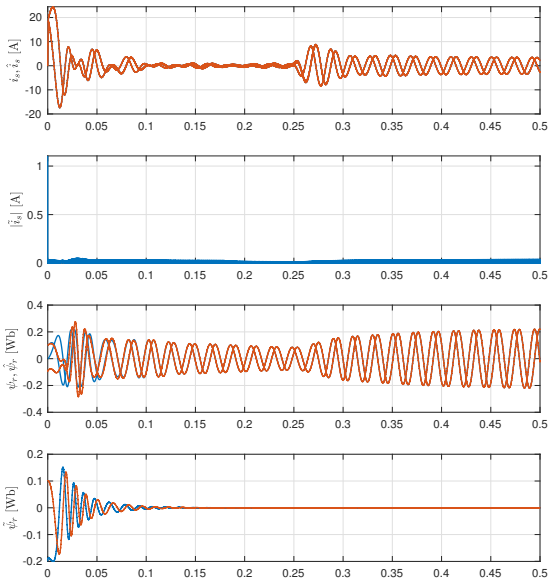

Fig. 4. Simulation results: Rotor-flux observation. From top to bottom: real and imaginary parts of the stator current (blue) and its observed values (red), $\hat{i}_s$, i_s; absolute error observation $|\tilde{i}_s|$; real and imaginary parts of the rotor flux (blue) and its observed values (in red), $\hat{\psi}_r$, ψ_r; real and imaginary components of the observation error, $\tilde{\psi}_r$.

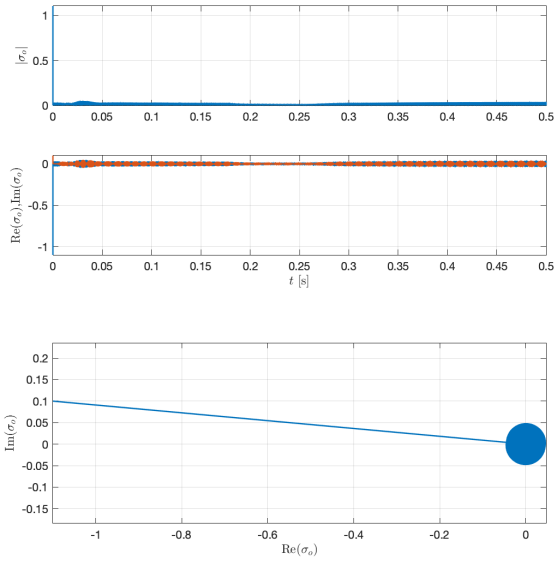

Fig. 5. Simulation results: Rotor-flux observation. From top to bottom: absolute value of the switching function, $|\sigma_o|$; real and imaginary parts of the switching function (in blue and red, respectively); complex plane plot of the switching function, σ_o.

proach, which is considerably different than the standard sliding modes, allows to tackle the control problem in the original $\alpha\beta$ coordinates without the use of additional reference frames. Although both the sliding manifold and the remaining sliding dynamics turn to be highly nonlinear, the complex description simplifies the analysis.

REFERENCES

Bachman, G. and Narici, L. (1966). *Functional Analysis*. Academic Press, INC, NY.

Baesmat, H.J. and Bodson, M. (2019). Pole placement control for doubly-fed induction generators using compact representations in complex variables. *IEEE Trans. on Energy Conversion*, 34(2), 750–760.

Bodson, M. (2019). Speed control for doubly fed induction motors with and without current feedback. *IEEE Trans. on Control Systems Technology (Early Access)*.

Chiasson, J. (2005). *Modeling and High Performance Control of Electric Machines*. Wiley, New York.

Dòria-Cerezo, A. and Bodson, M. (2016). Design of controllers for electrical power systems using a complex root locus method. *IEEE Trans. on Industrial Electronics*, 63(6), 3706–3716.

Dòria-Cerezo, A., Bodson, M., Batlle, C., and Ortega, R. (2013). Study of the stability of a direct stator current controller for a doubly-fed induction machine using the complex Hurwitz test. *IEEE Trans. on Control Systems Technology*, 21(6), 2323–2331.

Dòria-Cerezo, A., Serra, F., and Bodson, M. (2019). Complex-based controller for a three-phase inverter with an LCL filter connected to unbalanced grids. *IEEE Trans. on Power Electronics*, 34(4), 3899–3908.

Drakunov, S. and Utkin, V. (1995). Sliding mode observers. Tutorial. In *Proc. 34th Conference on Decision and Control*.

Harnefors, L. (2007). Modeling of three-phase dynamic systems using complex transfer functions and transfer matrices. *IEEE Trans. on Industrial Electronics*, 54(4), 2239–2248.

Holakooie, M., Ojaghi, M., and Taheri, A. (2019). Modified DTC of a six-phase induction motor with a second-order sliding-mode MRAS-based speed estimator. *IEEE Trans. on Power Electronics*, 34(1), 600–611.

Leonhard, W. (2001). *Control of electrical drives*. Springer, 3rd edition.

Morawiec, M. and Lewicki, A. (2019). Application of sliding switching functions in backstepping based speed observer of induction machine. *IEEE Trans. on Industrial Electronics (Early Access)*.

Novotny, D.W. and Lipo, T.A. (1996). *Vector Control and Dynamics of AC Drives*. Oxford Univ. Press, London, U.K.

Novotny, D. and Wouterse, J.H. (1976). Induction machine transfer functions and dynamic response by means of complex time variables. *IEEE Trans. on Power Apparatus and Systems*, 95(4), 1325–1335.

Utkin, V., Guldner, J., and Shi, J. (1999). *Sliding Mode Control in Electro-Mechanical Systems*. CRC Press.

Wang, B., Dong, Z., Yu, Y., Wang, G., and Xu, D. (2018). Static-errorless deadbeat predictive current control using second-order sliding-mode disturbance observer for induction machine drives. *IEEE Trans. on Power Electronics*, 33(3), 2395–2403.